iomac
International Operational Modal Analysis Conference

11th International Operational Modal Analysis Conference

20 - 23 May 2025 | Rennes, France

Analysis of brake squeal using the Harmonic Balance Vector (HBV) signal model: dependence of squeal frequency, fundamental and harmonic shapes on operational parameters

Guillaume Martin [1], *Etienne Balmes* [1,2], *Guilherme Malacrida Alves* [2] *and Guillaume Vermot des Roches* [1]

[1] SDTools, martin@mail.sdtools.com, balmes@mail.sdtools.com, vermot@mail.sdtools.com

[2] ENSAM, CNRS, CNAM, PIMM, etienne.balmes@ensam.eu

ABSTRACT

Brake squeal is a friction induced instability leading to limit cycle vibrations associated to a mode coupling. To analyze in detail this non-linear time varying phenomenon, a test campaign of a full brake system has been performed on an industrial test bench.

The first objective of this campaign is to extract squeal features. Squealing conditions where the disk velocity is imposed, and the brake pressure slowly evolves are chosen. To extract squeal features from measurements, a Harmonic Balance Vector (HBV) signal model based on the squeal signal characteristics is proposed. HBV signal model parameters are identified using a demodulation technique, providing slow time evolution of squeal fundamental frequency, fundamental shape and harmonic shapes. The model relevance is confirmed by analyzing the difference between the measured and the identified signals.

The second objective is to evaluate the relationship between squeal and operating parameters. The pressure evolution during the measurement leads to a strong evolution of the squeal. The analysis of the identified HBV signal highlights shape evolution with frequencies. At some fixed pressures, intermittent squeal occurs. The growth/decay rate is computed from the HBV signal and an experimental root locus is shown.

System modes also contain lots of information about the system dynamics. The last objective is to perform Experimental Modal Analysis in braking conditions. For several fixed pressures, the system is excited using a shaker. Two strategies are analyzed: excitation with sine-chirps and with pseudo-random signal.

Keywords: Harmonic Balance Vector (HBV) signal model; non-linear time varying system, Harmonics, ODS, EMA, Parametric study, Operational conditions, Brake

1. INTRODUCTION

Brake squeal is a friction induced instability leading to limit cycle vibrations associated to a mode coupling [1]. This phenomenon has been analyzed experimentally [2–4], highlighting the complex behavior of this limit cycle. Top of Figure 1 shows a squeal spectrogram (accelerometer measurement) where pressure is slowly increased. On the left, the wide spectrogram higlights the main features: the fundamental squealing frequency slowly increases with brake pressure and higher harmonics are present. On the right, a zoom on a 5s time band shows a repeating pattern every 1.3s, which corresponds to a wheel revolution.

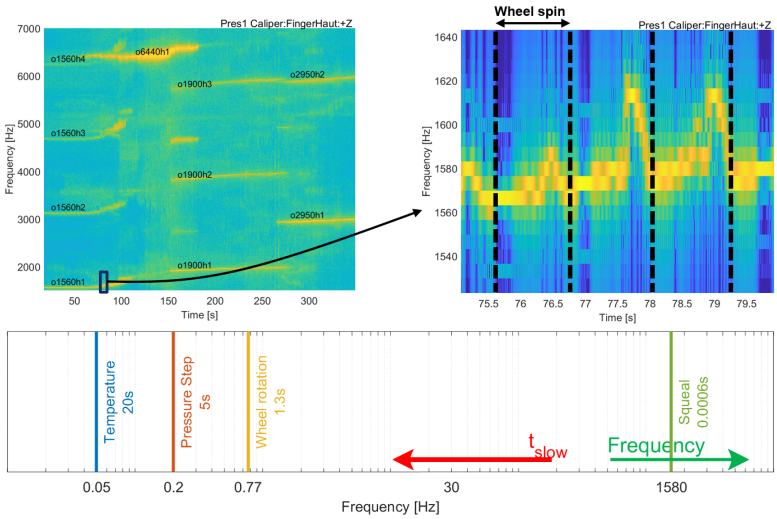

Figure 1: Squeal features: spectrograms (top) and time scales (bottom)

Despite a clear separation of time scales shown in the bottom of Figure 1, the spectrogram time-frequency compromise is here quite challenging: a narrow time sliding window (0.15s Hanning) is required to catch the evolution within the wheel revolution, leading to a poor frequency resolution (6.7 Hz). This motivated the introduction of the Harmonic Balanced Vector signal model, presented in Section 2., to properly extract squeal features from measurements.

The HBV signal model estimation is used in Section 3. to analyze the evolution of squeal features with brake pressure: frequency, shape and transitions between low and high vibration amplitude.

To extract information about the dynamics of the system apart from squealing, a shaker is used to add a controled excitation. Section 4. explores two strategies to build pressure dependant transfers.

The measurements used in this paper come from a test campaign of a full brake system performed on an industrial test bench in partnership with Hitachi Astemo France. The measurements used in this paper include vibration sensors (1 microphone and 17 accelerometers), 1 environment parameter (pad pressure) and 1 actuator (a shaker equipped with collocated force/acceleration sensor). The complete test campaign also contained 3D-SLDV and additional operating parameters (torque, temperature, disk/bracket distance, wheel speed,...) that will be analyzed in other publications.

2. HARMONIC BALANCED VECTOR SIGNAL MODEL : DEFINITION AND APPLICATION TO SQUEAL

The first objective is to build a signal model that captures the squeal features. From the Short Time Fourier Transform shown on top of Figure 1, the following signal characteristics are listed:

- Single fundamental frequency ω

- Superior harmonic frequencies $h\omega$ due to non-linearities
- Harmonic shapes $\{q_h\}_{N_s}$ (N_s sensors sharing the same harmonic frequencies)
- Slow time varying of frequency and shapes

The HBV signal model is inpired by the well-known analytic signal [5] which is a scalar complex signal of the form $a(t) = a_1(t)e^{i\varphi(t)} = a_1(t)e^{i\int_t \omega(t)dt}$ where the real part corresponds to the measured signal. The HBV signal model integrates the notion of shape (frequency common to all sensors) and harmonic frequencies, and makes explicit the slow time variation of frequency and shapes, leading to

$$\begin{aligned} \{q_{HBV}(\omega(t_{slow}), q_h(t_{slow}))\} = & \sum_{h\in\mathcal{H}} Re\left(\{q_h(t_{slow})\}\, e^{ih\varphi(t)}\right) \\ = & \sum_{h\in\mathcal{H}} Re\left(\{q_h(t_{slow})\}\, e^{ih\int_0^t \omega(t_{slow})dt}\right) \end{aligned} \tag{1}$$

The terminology has been chosen to emphasize the link with the Harmonic Balances Methods used in simulation to search periodic solutions of non-linear systems [6, 7], in particular for brake systems to find squeal limit cycle frequency and harmonic shapes.

To estimate this signal model from measurements, the synchronous demodulation technique commonly used in real time applications [8–10] will be used and adapted to tackle the specific characteristics of the HBV signal. Figure 2 shows the three-step algorithm proposed to estimate slow time varying frequency $\omega(t_{slow})$ and harmonic shapes $\{q_h(t_{slow})\}$ from the measured signal $\{q(t)\}$

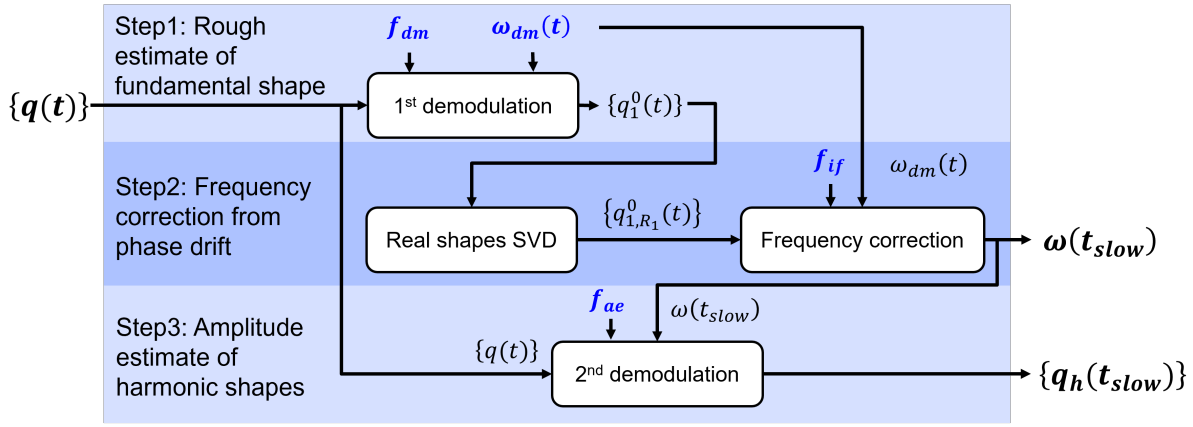

Figure 2: Three-step HBV signal model estimation algorithm

To estimate signal amplitude, synchronous demodulation requires a frequency which is unknown in the context of squeal measurement. Providing an initial guess of the frequency, a rough estimate of the fundamental shape is performed (step 1). The frequency being not exact, the resulting shape contains phase drift which is related to the frequency error, allowing to perform frequency correction (step 2). Now that the frequency is known with better accurency, a final demodulation allows to perform a finer estimation of the fundamental and higher harmonic shapes (step 3).

Step 1: Rough estimate of the fundamental shape

Figure 3 left illustrates the synchronous demodulation principle used in this first step. To understand this effect, let us first consider the simple scenario where a measured signal $q(t)$ is composed of a simple single harmonic $q_1(t_{slow})$ with constant frequency ω_0 of the form

$$\begin{aligned} q(t) = & \; Re(q_1(t_{slow})e^{i\omega_0 t}) = Re\left((q_{1c}(t) + iq_{1s}(t))e^{i\omega_0 t}\right) \\ = & \; q_{1c}(t)\cos(\omega_0 t) - q_{1s}(t)\sin(\omega_0 t) \end{aligned} \tag{2}$$

where the dependence on t_{slow} is dropped to alleviate notations. The product of the signal $q(t)$ with quadrature signals $2\cos(\varphi_{dm}(t))$ and $-2\sin(\varphi_{dm}(t))$ with the same constant frequency leading to phase $\varphi_{dm}(t) = \omega_0 t$ is

$$\begin{aligned} 2q(t)\cos(\omega_0 t) &= 2\left(q_{1c}(t)\cos(\omega_0 t) - q_{1s}(t)\sin(\omega_0 t)\right)\cos(\omega_0 t) \\ &= q_{1c}(t) - q_{1s}(t)\sin(2\omega_0 t) + q_{1c}(t)\cos(2\omega_0 t) \\ -2q(t)\sin(\omega_0 t) &= -2\left(q_{1c}(t)\cos(\omega_0 t) - q_{1s}(t)\sin(\omega_0 t)\right)\sin(\omega_0 t) \\ &= q_{1s}(t) - q_{1s}(t)\cos(2\omega_0 t) - q_{1c}(t)\sin(2\omega_0 t) \end{aligned} \tag{3}$$

and using a low pass filter allows to eliminate the $2\omega_0$ frequency component and leads to estimates of $q_{1c}(t)$ and $q_{1s}(t)$ and thus the complex amplitude $q_1(t)$.

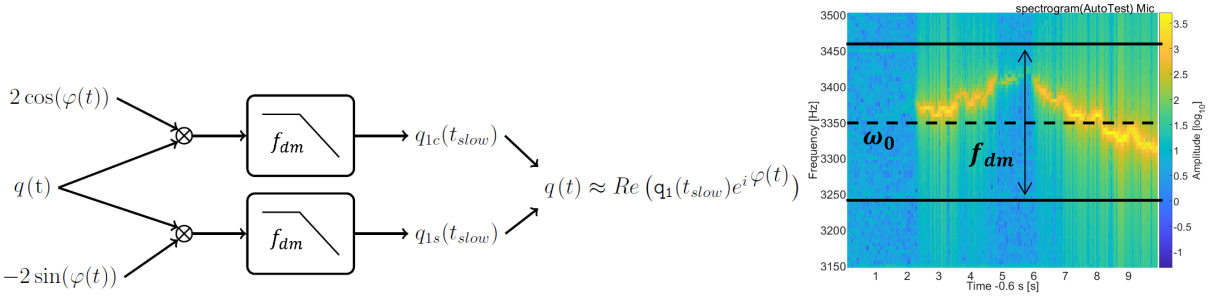

Figure 3: Synchronous demodulation algorithm (left), step1 parameter tuning on brake squeal spectrogram (right)

In the more general case of a measured signal with a varying frequency $\omega(t)$

$$q(t) = Re(q_1(t)e^{i\int_0^t \omega(t)dt}), \tag{4}$$

the synchronous demodulation using a phase $\varphi_{dm}(t) = \int_0^t \omega_{dm}(t)dt$ with $\omega_{dm}(t) \neq \omega(t)$ leads to a complex amplitude $q_1^0(t)$ containing a phase drift $\delta\varphi(t)$ related to the frequency error $\delta\omega(t) = \omega(t) - \omega_{dm}(t)$

$$\begin{aligned} q(t) &= Re(q_1(t)e^{i\int_0^t(\omega(t)-\omega_{dm}(t))dt}e^{i\int_0^t \omega_{dm}(t)dt}) \\ &= Re(q_1(t)e^{i\int_0^t \delta\omega(t)dt}e^{i\varphi_{dm}(t)}) \\ &= Re(q_1(t)e^{i\delta\varphi(t)}e^{i\varphi_{dm}(t)}) \\ &= Re(q_1^0(t)e^{i\varphi_{dm}(t)}) \end{aligned} \tag{5}$$

The phase drift $\delta\varphi(t)$ is related to the complex amplitude $q_1^0(t) = q_{1c}^0(t) + iq_{1s}^0(t)$ and the frequency error $\delta\omega(t)$

$$\delta\varphi(t) = tan^{-1}\left(\frac{q_{1s}^0(t)}{q_{1c}^0(t)}\right) = \int(\delta\omega(t)dt) = \int(\omega(t) - \omega_{dm}(t))dt \tag{6}$$

The varying frequency is thus retrived from

$$\omega(t) = \omega_{dm}(t) + \frac{d}{dt}\left(tan^{-1}\left(\frac{q_{1s}^0(t)}{q_{1c}^0(t)}\right)\right) \tag{7}$$

To capture this frequency error, as shown in Figure 3 right, step 1 requires

- an initial guess of the squeal frequency $\omega_{dm}(t)$ (here a constant frequency $\omega_{dm}(t) = \omega_0$)
- the low pass filter frequency f_{dm} to be higher than the frequency error, thus defining a frequency band where the squeal frequency is seeked

This demodulation being applied to N_s sensors, the output of step 1, the complex shape $\left\{q_1^0(t)\right\}$ contains as many frequency errors as sensors.

Step 2: Frequency correction from phase drift

To extract a unique frequency, step 2 proposes to apply the frequency correction (7) to the complex generalized amplitude associated to the first principal real shape of the demodulated signals $\left[q_1^0(t)\right]_{N_S \times N_T}$ (step 1). To obtain real principal shapes (N_S sensors) associated to complex amplitudes (time evolution with N_T time steps), the real and imaginary parts are reordered sequentially and Singular Value Decomposition is performed, leading to

$$\begin{array}{rcl} \left[q_{1c}^0(t) \quad q_{1s}^0(t)\right]_{N_S \times (2N_T)} & = & \sum_j \left\{u_j\right\}_{N_S \times 1} \left(\sigma_j \left\{v_{jc}^T \quad v_{js}^T\right\}\right)_{1 \times 2N_T} \\ & = & \sum_j \left\{u_j\right\} \left\{q_{1c,R_j}(t) \; q_{1s,R_j}(t)\right\} \end{array} \tag{8}$$

Each $\{u_j\}$ principal real shape is associated to a generalized amplitude vector $\left\{q_{1c,R_j}(t) \; q_{1s,R_j}(t)\right\}$ that is approriately reordered as a complex generalized amplitude $\left\{q_{1,R_j}(t)\right\} = \left\{q_{1c,R_j}(t)\right\} + i\left\{q_{1s,R_j}(t)\right\}$ to obtain the desired decomposition

$$\left[q_1^0(t)\right]_{N_S \times (2N_T)} = \sum_j \left\{u_j\right\}_{N_S \times 1} \left\{q_{1,R_j}(t)\right\}_{1 \times N_T} \tag{9}$$

R_j indexing is used to indicate the fact that this corresponds to a reduction of the signal dimension.

Figure 4 shows in blue the estimation of the instantaneous frequency $\omega(t)$ obtained from applying equation (7) to the first complex generalized amplitude $\{q_{1,R_1}(t)\}$. The result is quite noisy because of the derivation and does not satisfy the slowly varying assumption required in the signal model (1). A low pass filter with cutoff frequency f_{if} is thus applied leading to the smoother red curve.

$$\omega(t_{slow}) = LP_{f_{if}}\left(\omega_{dm}(t) + \frac{d}{dt}\left(tan^{-1}\left(\frac{q_{1s}^0(t)}{q_{1c}^0(t)}\right)\right)\right) \tag{10}$$

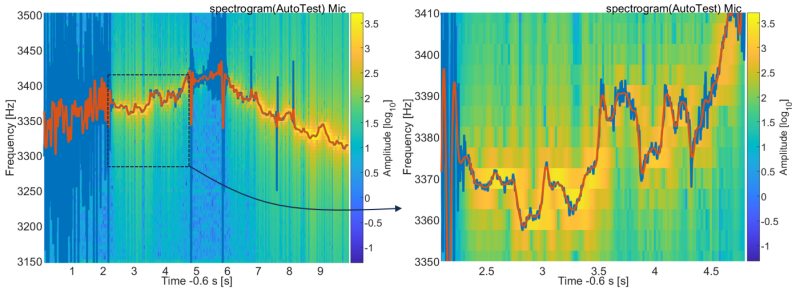

Figure 4: Instantaneous frequency correction: without (blue) and with (red) low pass filtering

Step 3: Amplitude estimate of harmonic shapes

Once the instanteneous frequency $\omega(t_{slow})$ is known with better accuracy (step 2), the last step consists in h demodulations of the measured signal $\{q(t)\}$ with the phases $\varphi_h(t) = \int_0^t h\omega(t_{slow})dt$ corresponding to each harmonic. The demodulation low pass filter f_{ae} is lower than f_{dm} used in step 1, because the frequency error $\delta\omega(t)$ is expected to be small. These demodulations lead to the estimation of the harmonic shapes $\{q_h(t_{slow})\}$.

The relevance of applying the algorithm to squeal measurements is highlighted by Figure 5. The spectrogram of the microphone measurement is shown on the left. The time evolution of the instantaneous frequency $\omega(t_{slow})$, with color correponding to the time evolution of the amplitude $q_1(t_{slow})$ is show in the middle. Finally, the spectrogram of the difference between raw time data and the estimated HBV signal for this sensors is shown on the right: it remains almost only noise.

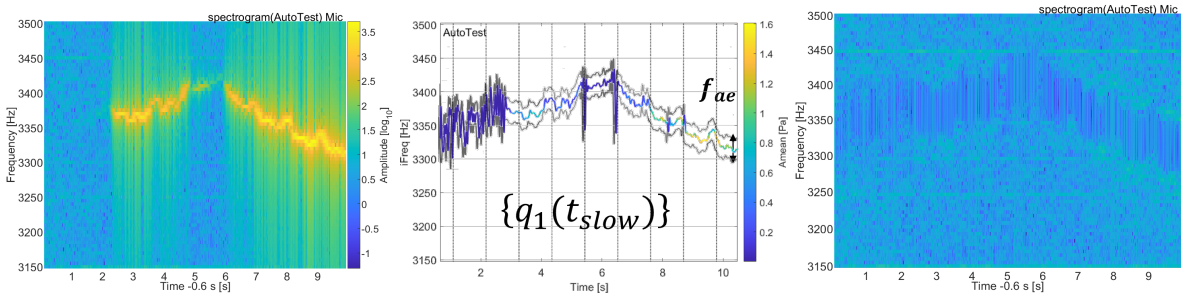

Figure 5: HBV signal model estimation through demodulation : raw measurement spectrogram (left), instantaneous frequency estimating through demodulation (middle) and spectrogram of the signal reminder (right)

3. EVOLUTION OF SQUEAL FEATURES WITH BRAKE PRESSURE

The second objective of the paper is to evaluate the relationship between squeal and the brake pressure. One measurement where the disk velocity is imposed, and the brake pressure slowly evolves is chosen, with squeal occurring in the [15-10] Bar pressure range. The HBV signal estimation is performed from the 17 accelerometer measurements and Figure 6 shows how the identified squeal characteristics evolve. Figure 6 left shows that squeal appears with intermittence at P=15bar. It is rather permanent in the [14-11] bar pressure range and disappears with intermittence at P=10bar. Figure 6 middle highlights that squeal frequency decreases when pressures deacreases. A periodic pattern every 2.5s in Figure 6 left and middle is visible, it corresponds to the time of a wheel revolution.

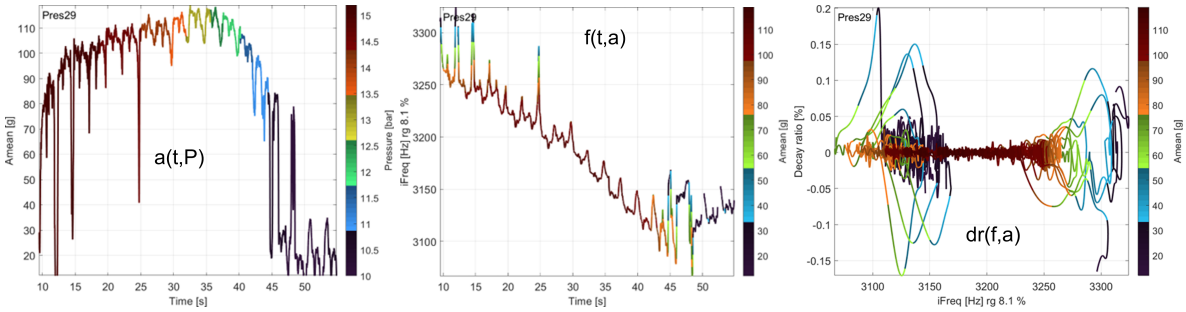

Figure 6: Squeal amplitude as function of time and pressure (left), squeal freqeuncy as function of time and amplitude (middle), squeal decay ratio as function of frequency and amplitude (experimental root locus, right)

To analyze in more detail the growing and decaying phase in intermitent squeal, the decay ratio is defined using an amplitude estimate $A(t_{slow})$, the principal coordinate (9) or the norm of the HBV vector

$$\{\zeta_{DR}(t)\} = -\frac{1}{\omega(t_{slow})}\frac{d}{dt}(log(A(t_{slow}))) \tag{11}$$

Note that this would correspond to the damping ratio if $A(t_{slow})$ was a modal amplitude of a second order system. Figure 6 right highlights that amplitude growth (negative decay ratio) comes with a frequency increase and amplitude decay (positive decay ratio) comes with a frequency decrease.

To analyze the evolution of squeal shape, the HBV signal is decomposed into main real shapes using (9). Figure 7 left shows that two real shapes are mainly present. Taking the first generalized coordinate $q_{1,R_1}(t_{slow})$ as reference, Figure 7 right shows the amplitude ratio $|q_{1,R_2}(t_{slow})/q_{1,R_1}(t_{slow})|$ and the phase difference $tan^{-1}(q_{1,R_2}(t_{slow})/q_{1,R_1}(t_{slow}))$ evolving with pressure instantaneous frequency and pressure (color). In the permanent squeal time window P=[14-12] Bar (t=[15-40]s), the second shape amplitude grows with pressure, up to becoming predominant at highest pressure. The phase difference between the two real shapes is fairly stable around -90°. At low (11-12 bar) and high (15 bar) pressure, squeal is intermittent which explains the horizontal spread in Figure 7 right. The study of these transition

zones would require a more detailed analysis, as the contributions of the other shapes are no longer negligible.

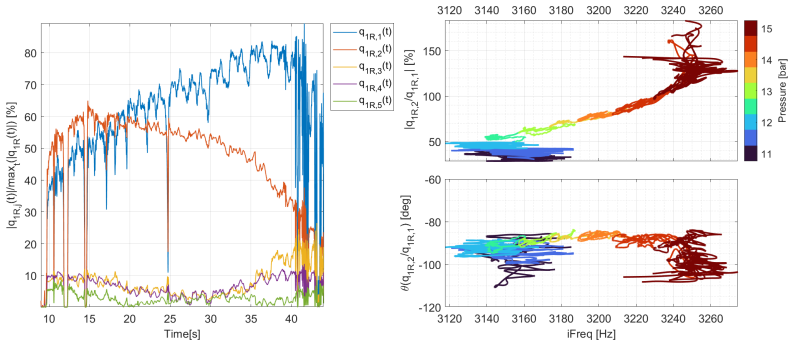

Figure 7: Evolution of main real shape participation to squeal (left) and evolution with frequency and pressure of the two first generalized coordinates (amplitude ratio and phase difference, right)

4. EXPERIMENTAL MODAL ANALYSIS IN BRAKING CONDITIONS: PRESSURE DEPENDENCE AND LINK WITH SQUEAL

System modes also contain lots of information about the system dynamics. The last objective is to perform Experimental Modal Analysis in braking conditions. For several fixed pressures, the system is excited using a shaker. Two strategies are analyzed: excitation with sine-chirps and with pseudo-random signal. Figure 8 left shows that close the the squeal but in stable condition, a resonance is visibleat 3100Hz with a good coherence. Despite repeatability issues, EMA could be performed to provide mean frequency, damping and shape. When squeal appears at 9bar, Figure 8 right show an amplitude and phase dropt in the band [3150-3200] were the squeal lies at this pressure. The coherence is bad in this frequency band because of the internal force at the pad/disc sliding interface that causes the squeal: EMA cannot be performed.

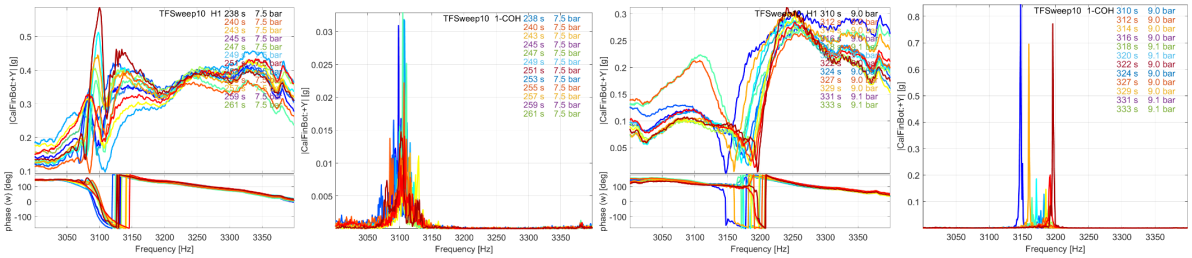

Figure 8: Transfer estimation with sine chirps: repetitions at 7.5 bar, transfers and 1-coherence (left); repetitions at 9 bar, transfers and 1-coherence (right)

The repeatability isue is probably due to the squeal dependance to the wheel position while the sine-chirps are not synchronized with the wheel rotation. To see mode evolution during a wheel revolution, pseudo-random excitation is proposed with multiple sinus frequencies in the band $[3000 - 3400]$ Hz, each 10Hz apart. This signal is periodic in a 0.1s time window so that transfer estimation is performed by computing the ratio between sliding Fourier Transform of the output accelerometers and the sliding Fourier Transform of the input force. Figure 9 shows a the fixed pressures the evolution of the transfer with time: we see the periodic patterns every 7s which corresponds to wheel revolution period. Slices in a wheel revolution at fixed pressure P=7.5bar shows the transition between a more damped mode around 3150Hz and a less damped mode around 3100Hz. At fixed pressure P=9bar, the squeal does not appear anymore with the pseudo random excitation (non-linear pad/disc sliding contact force is working differently, which may prevent the instability to occur?): we see in a wheel revolution transitions between two modes around 3080Hz and 3270Hz and a higher amplitude mode around 3180Hz.

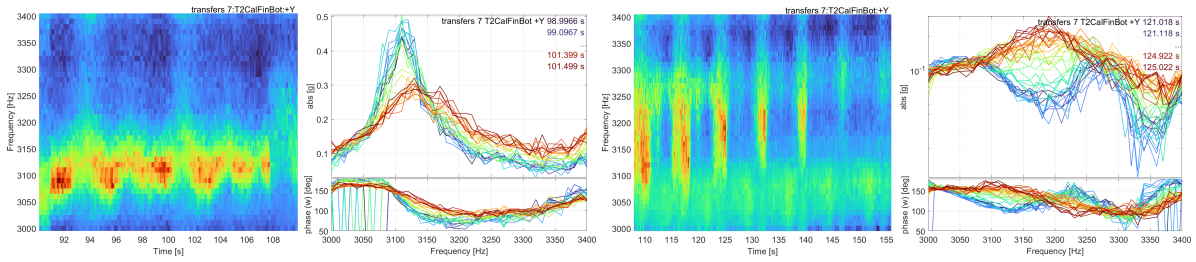

Figure 9: Transfer estimation with pseudo-random signal: transfer evolution at 7.5 bar and slices in a wheel revolution (left); transfer evolution at 9 bar and slices in a wheel revolution (right)

A third excitation strategy with a sinusoid whose frequency is controlled to track the mode of interest should be tested: it would allow to analyze its evolution during the wheel revolution while making the non-linear pad/disc sliding contact force working in a similar manner than squeal does.

5. CONCLUSION

This paper introduces the HBV signal model to represent squeal characteristics: slow time evolution of instantaneous frequency $\omega(t_{slow})$ and harmonic shapes $\{q_h(t_{slow})\}$. A three-step estimation algorithm is proposed and its relevance is confirmed: when the estimated signal is subtracted from the raw measurement, virtually all that remains is noise. This HBV signal is very helpful to analyze transitions of squeal features (frequency, harmonic shapes) and resulting indicators (amplitude, decay ratio, main real shapes) with pressure. Two strategies have been explored to build transfers in operating conditions, using sine-chirps and pseudo-random signals. Both lead to comparable but different results and further investigation is required.

ACKNOWLEDGMENTS

The authors deeply thank Hitachi Astemo France for partial funding and for the authorization to use their dyno bench and acquisition system during two weeks, allowing to perform the test campaign. Tests have been performed on a brake design chosen for its high propensity to squeal and is not representative of production brakes.

REFERENCES

[1] Frank Moirot. *Etude de La Stabilité d'un Équilibre En Présence de Frottement de Coulomb*. PhD thesis, Ecole Polytechnique, 1998.

[2] Francesco Massi, Oliviero Giannini, and Laurent Baillet. Brake squeal as dynamic instability: An experimental investigation. *The Journal of the Acoustical Society of America*, 120(3):1388–1398, September 2006. ISSN 0001-4966. doi: 10.1121/1.2228745.

[3] Merten Stender, Merten Tiedemann, Lando Hoffmann, and Norbert Hoffmann. Determining growth rates of instabilities from time-series vibration data: Methods and applications for brake squeal. *Mechanical Systems and Signal Processing*, 129, April 2019. doi: 10.1016/j.ymssp.2019.04.009.

[4] Guillaume Martin, Etienne Balmes, Guillaume Vermot Des Roches, and Thierry Chancelier. Squeal measurement with 3D Scanning Laser Doppler Vibrometer: Handling of the time varying system behavior and analysis improvement using FEM expansion. In *ISMA*. KUL, September 2018.

[5] Michael Feldman. Hilbert transform in vibration analysis. *Mechanical Systems and Signal Processing*, 25(3):735–802, April 2011. ISSN 08883270. doi: 10.1016/j.ymssp.2010.07.018.

[6] N. Coudeyras, J. J. Sinou, and S. Nacivet. A new treatment for predicting the self-excited vibrations of nonlinear systems with frictional interfaces: The Constrained Harmonic Balance Method, with application to disc brake squeal. *Journal of Sound and Vibration*, 319(3-5):1175–1199, January 2009. ISSN 0022-460X. doi: 10.1016/j.jsv.2008.06.050.

[7] Javad Taghipour, Hamed Haddad Khodaparast, Michael I. Friswell, Alexander D. Shaw, Hassan Jalali, and Nidhal Jamia. Harmonic-Balance-Based parameter estimation of nonlinear structures in the presence of Multi-Harmonic response and force. *Mechanical Systems and Signal Processing*, 162:108057, January 2022. ISSN 0888-3270. doi: 10.1016/j.ymssp.2021.108057.

[8] Solomon Davis and Izhak Bucher. Automatic vibration mode selection and excitation; combining modal filtering with autoresonance. *Mechanical Systems and Signal Processing*, 101:140–155, February 2018. ISSN 08883270. doi: 10.1016/j.ymssp.2017.08.009.

[9] Maren Scheel. Nonlinear modal testing of damped structures: Velocity feedback vs. phase resonance. *Mechanical Systems and Signal Processing*, 165:108305, February 2022. ISSN 0888-3270. doi: 10.1016/j.ymssp.2021.108305.

[10] Cédric Peeters, Jérôme Antoni, Quentin Leclère, Timothy Verstraeten, and Jan Helsen. Multi-harmonic phase demodulation method for instantaneous angular speed estimation using harmonic weighting. *Mechanical Systems and Signal Processing*, 167:108533, March 2022. ISSN 08883270. doi: 10.1016/j.ymssp.2021.108533.